

1 **Quantifying Background Nitrate Removal Mechanisms in an Agricultural Watershed with**  
2 **Contrasting Subcatchment Base-flow Concentrations**

3

4 Wesley O. Zell<sup>1</sup> (wzell@usgs.gov) \*corresponding author

5 Teresa B. Culver<sup>2</sup> (tbc4e@virginia.edu)

6 Ward E. Sanford<sup>1</sup> (wsanford@usgs.gov)

7 Jonathan L. Goodall<sup>2</sup> (goodall@virginia.edu)

8 <sup>1</sup> U.S. Geological Survey, 12201 Sunrise Valley Dr, MS 432, Reston, VA 20192

9

10 <sup>2</sup> Department of Civil and Environmental Engineering, University of Virginia, Thornton Hall, P.O.  
11 Box 400259, Charlottesville, VA 22904-4259

12

13 The authors declare no competing interests.

14

**15 ABSTRACT**

16 Numerous studies have documented the linkages between agricultural nitrogen loads and  
17 surface water degradation. In contrast, potential water quality improvements due to  
18 agricultural best management practices are difficult to detect because of the confounding  
19 effect of background nitrate removal rates as well as the groundwater-driven delay between  
20 land surface action and stream response. To characterize background controls on nitrate  
21 removal in two agricultural catchments we calibrated groundwater travel time distributions  
22 with subsurface environmental tracer data to quantify the lag time between historic  
23 agricultural inputs and measured base-flow nitrate. We then estimated spatially-distributed  
24 loading to the water table from nitrate measurements at monitoring wells, using machine  
25 learning techniques to extrapolate the loading to unmonitored portions of the catchment in  
26 order to subsequently estimate catchment removal controls. Multiple models agree that in-  
27 stream processes remove as much as 75% of incoming loads for one subcatchment while  
28 removing less than 20% of incoming loads for the other. The use of a spatially variable loading  
29 field did not result in meaningfully different optimized parameter estimates or model  
30 performance when compared to spatially constant loading derived directly from a county-scale  
31 agricultural nitrogen budget. While previous studies using individual well measurements have  
32 shown that subsurface denitrification due to contact with a reducing argillaceous confining unit  
33 plays an important role in nitrate removal, the catchment-scale contribution of this process is  
34 difficult to quantify given the available data. Nonetheless, the study provides a baseline  
35 characterization of nitrate transport timescales and removal mechanisms that will support  
36 future efforts to detect water quality benefits from ongoing BMP implementation.

## 37 **1 INTRODUCTION**

38 Numerous studies have documented the linkages between agricultural nitrogen loads and  
39 surface water degradation (Vitousek et al., 1997; Schindler and Vallentyne, 2008). The adverse  
40 effects of excess dissolved nitrate include the seasonal dissolved oxygen deficits and algal  
41 blooms that persist in many bays and estuaries despite widespread implementation of  
42 agricultural best management practices (BMPs) in upstream catchments. This persistence is  
43 due to the ongoing discharge of groundwater nitrates that have accumulated in surficial  
44 aquifers during the past century (Puckett et al., 2011). For example, in some agriculturally  
45 intensive regions of the Chesapeake Bay watershed as much as 70% of nitrate loads are  
46 delivered to the Bay or its tributaries as groundwater discharge (Lindsey et al., 2003, Ator and  
47 Denver, 2012; Sanford and Pope, 2013).

48 While loading reductions and water quality improvement due to BMPs have been  
49 documented at laboratory and field scales (e.g., Staver and Brinsfield, 1998), the anticipated  
50 effects of these practices are often difficult to detect at the outlets of agricultural watersheds in  
51 which they have been widely implemented (Osmond et al., 2012; Meals et al., 2010). This  
52 difficulty is in part due to the lag time between land surface action and surface water response  
53 that results from groundwater transport pathways (Sanford and Pope, 2013; Tesoriero et al.,  
54 2013; Science and Technical Advisory Committee, 2005). However, the effects of BMPs are also  
55 difficult to disentangle from other spatially and temporally distributed factors affecting in-  
56 stream loads (Gitau et al., 2010; Sutton et al., 2009). These factors, which may vary widely  
57 between catchments, include background rates of nitrogen removal at the land surface, in the  
58 aquifer, or in the receiving stream (Meals et al., 2010; Böhlke and Denver, 1995).

59       The objective of the study described in this paper was to differentiate and quantify long-  
60 term, catchment-integrated nitrate removal mechanisms in two adjacent agricultural  
61 headwater catchments with similar contributing land use histories but contrasting stream  
62 nitrate concentrations. While the fate and transport of agricultural nitrate has been widely  
63 investigated, there have been few if any studies that characterize long-term effects of  
64 subsurface or in-stream nitrate removal in a highly spatially variable system. For example,  
65 many studies have examined the short-term (1-5 year) groundwater-driven discharge of  
66 agricultural nitrates to headwater streams with goals of differentiating seasonally variable  
67 nitrate sources (Yevenes and Mannaerts, 2012) or identifying changes in hydrologic  
68 connectivity between uplands and discharge areas (Petry et al., 2002; Wriedt et al., 2007;  
69 Molenat et al., 2008). For the characterization of in-stream nitrate variability at these shorter  
70 time scales, it is not necessary to account for the full, multi-decadal loading history, and it is  
71 common to treat upgradient catchment nitrate as an effectively steady-state reservoir draining  
72 subject to hydrological controls (Vidon and Hill, 2004; Montreuil et al., 2010). While some  
73 studies have directly measured in-stream rates of nitrogen removal for headwater catchments  
74 (Royer et al., 2004; Vidon and Hill, 2004; Mulholland et al., 2008), questions remain about  
75 extrapolating these measurements to larger spatial and temporal scales (Boyer et al, 2002).  
76 Few groundwater studies have examined the long-term behavior of agricultural nitrogen inputs  
77 and export. Aquilina et al. (2012) used groundwater nitrate and chlorofluorocarbon (CFC)  
78 measurements to reconstruct the long-term nitrate input function for a catchment in Brittany  
79 (France); they simulated long-term in-stream nitrate concentrations at the catchment outlet

80 but assumed conservative export and did not investigate removal processes. Sanford and Pope  
81 (2013) combined groundwater travel times from a calibrated regional simulation with a  
82 regression method to estimate spatially constant nitrate removal terms for the Delmarva  
83 Peninsula (USA); however, the scale of their investigation did not allow for spatial variation of  
84 removal terms or the effects of catchment-scale hydrogeological variability. A few studies have  
85 documented the potential of catchment-scale, physics-based simulation of nitrate fate and  
86 transport through coupled landscape-groundwater-surface water systems (Conan et al., 2003;  
87 Galbiati et al., 2006; Wei et al., 2018), but these simulations are likewise limited to short time  
88 scales and subsurface linkages are not constrained by environmental tracer data.

89 To address these knowledge gaps we leveraged a multi-decadal record of catchment nitrate  
90 inputs and exports as well as a unique dataset of environmental tracer measurements,  
91 groundwater nitrate measurements, and in-stream nitrate measurements to simulate long-  
92 term average nitrate controls for adjacent headwater streams. We use a fully distributed,  
93 three-dimensional numerical simulation of the groundwater system to link land surface inputs  
94 to subsurface and in-stream nitrate concentrations, and we examined the significance of  
95 spatially distributed representation of catchment nitrate loading for parameter estimation and  
96 uncertainty.

## 97 **2 MATERIALS AND METHODS**

### 98 **2.A Overview of Study Site**

99 The 61-km<sup>2</sup> study site (hereafter referred to as the 'Upper Chester' - cf. Nelson and Spies,  
100 2013) is in Kent County, MD, and is a low-relief agricultural watershed drained by small gaining

101 streams; the Chesterville Branch (USGS gage 1493112) and Morgan Creek (USGS gage 1493500)  
102 subcatchments are the focus of this paper (**Figure 1**). These subcatchments have similar land-  
103 use histories, soil types, and stream discharge rates but widely different in-stream nitrate  
104 levels. Water quality throughout the Upper Chester deteriorated during the last century due to  
105 agricultural intensification and elevated fertilizer inputs (**Figure 2**; cf. Böhlke and Denver, 1995).  
106 In recent years, a variety of management practices aimed at damping adverse agricultural  
107 effects and improving water quality have been implemented in the Upper Chester (Nelson and  
108 Spies, 2013). Concentrations at the Morgan Creek stream gage ranged between 2 and 3 mg  
109 NO<sub>3</sub>-N/L for the duration of its sampling history; in contrast, concentrations at the Chesterville  
110 Branch stream gage have increased from 4-6 mg/L in the early 1990s and currently persist near  
111 10 mg/L (**Figure 3**).

112 **Insert Figure 1**

113 **Insert Figure 2**

114 **Insert Figure 3**

115 Previous studies in Morgan Creek suggest several potential reasons for the disparity in  
116 mean baseflow nitrate concentration though no catchment-scale studies have integrated the  
117 available data and quantified their relative contributions. Böhlke and Denver (1995) found  
118 evidence of denitrification (elevated nitrate  $\delta^{15}\text{N}$  levels, excess dissolved N<sub>2</sub>, and indicators of  
119 pyrite reduction) due to a glauconitic confining unit that outcrops at the lower reaches of  
120 Morgan Creek (**Figure 1**). Bachman et al. (2002) observed increasing silica concentrations in a

121 downstream direction on Morgan Creek. Groundwater silica concentrations elsewhere on the  
122 Delmarva Peninsula have been shown to positively correlate with tritium-derived groundwater  
123 ages (Clune and Denver, 2012), such that increased silica in the lower reaches of Morgan Creek  
124 may indicate the dilution of agricultural nitrates with older, higher silica, nitrate-free  
125 groundwater that reaches the stream from the lower confined aquifer. Sediment cores in  
126 lower Morgan Creek show an abrupt change in the elevation of the confining unit and thus  
127 suggest a discontinuity that could allow influx of older groundwater from the deeper, confined  
128 aquifer (Bachman et al., 2002). Finally, because the Morgan Creek stream channel is downcut  
129 into the low-permeability confining unit, direct groundwater discharge through the streambed  
130 is limited, and groundwater instead emerges through seeps at the edge of a near-stream  
131 floodplain before traveling to the main channel via small rivulets and sheetflow; Duff et al.  
132 (2008) observed decreasing nitrate concentrations in the groundwater, rivulets, and stream,  
133 respectively, for lower Morgan Creek, suggesting the importance of riparian nitrogen removal.

134 Chesterville Branch has not been investigated with the same detail as Morgan Creek.  
135 However, the higher-permeability surficial sediments are much deeper under Chesterville  
136 Branch than Morgan Creek (Böhlke and Denver, 1995), suggesting that a higher percentage of  
137 base-flow discharge bypasses nitrate removal mechanisms in the riparian zone (Zell et al.,  
138 2018). Similar bypasses, and their importance for nitrate processing, have been noted in other  
139 agricultural systems (e.g., Tesoriero et al., 2013; Vidon and Hill, 2004).

## 140 **2.B Simulation of Groundwater Flow and Nitrate Transport**

141 In a separate study we document the development, calibration, and sensitivity/uncertainty  
142 analysis of several candidate numerical flow and transport simulation models for the Upper  
143 Chester (Zell et al., 2018). The models represent a range of plausible interpretations of the  
144 Upper Chester groundwater system and simulate steady-state subsurface flow and advective  
145 solute transport using the US Geological Survey (USGS) finite-difference code MODFLOW  
146 (Harbaugh, 2005) and its companion particle-tracking software MODPATH (Pollock, 2012). For  
147 each model, spatially variable recharge, horizontal hydraulic conductivity, anisotropy, and  
148 porosity were calibrated against groundwater levels, base-flow discharge, and more than 200  
149 subsurface measurements of atmospherically derived age tracers.

150 For the present study, we selected the two best performing flow and transport models and  
151 used them to (i) generate flux-weighted travel time distributions (TTD) at nitrate monitoring  
152 locations and (ii) identify the associated contributing recharge area for each nitrate monitoring  
153 location in the study area (i.e., monitoring wells and the Chesterville Branch and Morgan Creek  
154 catchment outlets). In the remainder of the manuscript we refer to these TTD models as the  
155 nitrate transport ‘base models’. The selected base models are chiefly differentiated by  
156 assumptions about base-flow indices (BFI) in the Upper Chester and are consequently labeled  
157 ‘LowBFI’ and ‘HighBFI’ (see Zell et al., 2018, for more details). Given the TTDs provided by these  
158 base models, the concentration of a solute at a monitoring location  $j$  may be calculated by the  
159 convolution of a TTD with the time series of solute inputs to the catchment, expressed in its  
160 discrete form as



$$C_j[t] = \sum_{\tau=0}^{\infty} C[x,y,t-\tau]g_j[\tau] \quad , \quad (1)$$

161 where  $C(x,y,t-\tau)$  is the solute (e.g., dissolved nitrate) input signal and  $g_j(\tau)$  is the flux-  
162 weighted TTD of groundwater sampled at  $j$ .

## 163 2.C Estimation of nitrate loading to the water table

164 As an initial estimate of nitrate inputs to the water table (i.e.,  $C(x,y,t-\tau)$  in **Equation 1**) we  
165 calculated a county-level nitrogen budget for the years 1930-2015 using Kent County (MD)  
166 agricultural data and nitrogen wet deposition data for the Maryland Eastern Shore (**Figure 2**).  
167 In the remainder of the paper we refer to this spatially constant, county-scale time series as the  
168 ‘reference loading’. We then calibrated multiple sets of spatially variable loading factors that,  
169 when applied to the reference loading time series, resulted in a range of estimates of the  
170 temporally and spatially variable flux of nitrate across the water table. Loading factors were  
171 estimated by calibrating the nitrate transport model (**Equation 1**) solely against observed  
172 groundwater nitrate concentrations under different calibration scenarios that varied with  
173 respect to both the base flow and transport model as well as the weighting scheme applied to  
174 the nitrate observation dataset (**Table 1** and Supplemental Materials Section **S1**).

### 175 **Insert Table 1**

176 Due to the generally oxic character of the subsurface and the expected conservative nitrate  
177 transport from the water table to observation wells, we assumed that most groundwater  
178 nitrate concentrations in the Upper Chester provide direct information about nitrate loading to  
179 the water table (i.e., after nitrate removals such as crop export or soil denitrification) (Green et

180 al., 2010). However, while groundwater nitrate observations in the Upper Chester are  
181 abundant when compared to many sites, monitoring well nitrate data only constrain a portion  
182 of the model domain. Each stage 1 scenario therefore included use of a Gradient Boosted  
183 Regression (GBR) method to extrapolate the calibrated water table loading factors from the  
184 monitored subdomain to the entire model area on the basis of proxy relationships with other  
185 mapped data. These candidate explanatory variables included soils and land use data derived  
186 from national-scale datasets as well as estimates of hydrologic states and system properties  
187 developed during this study. The GBR methods and results are fully described in the  
188 Supplemental Materials.

## 189 **2.D Estimation of catchment nitrate removal**

190 In the second stage of parameter estimation, we used the stage 1 scenarios as a range of  
191 possible loadings and estimated nitrate removal at the confining unit and in/near each stream  
192 by calibrating the resulting nitrate transport models against base-flow nitrate observations.  
193 Base-flow nitrate concentrations were considered to be those measurements associated with a  
194 stream discharge observation for which the separated base-flow was more than 85% of total  
195 flow (using the digital filter separation method of Arnold et al., 1995) (**Figure 3**).

196 As discussed in the development of the flow and transport base models, uncertainties about  
197 the spatial distribution of catchment hydraulic conductivity, porosity, and recharge propagate  
198 through to the simulated base-flow TTDs (Zell et al., 2018). Therefore, while the base-flow TTDs  
199 used in this study are relatively well-constrained by hydraulic and atmospheric tracer data, it is  
200 expected that they may be updated by conditioning them upon stream nitrate data. We

201 consequently allowed the calibration to adjust the TTDs by means of stream-specific scaling  
202 factors that may improve the simulation of base-flow nitrate trends. Note also that, for  
203 purposes of evaluating model uncertainty, the inclusion of TTD scaling parameters is a means of  
204 remedying non-conservative uncertainty estimates that result from assuming that base-flow  
205 travel times are known.

206 Due to correlations between stream removal and confining unit removal in Morgan Creek it  
207 was assumed that fixing the confining unit parameter value (and thus routing all available  
208 stream nitrate information to the stream removal parameters) would reduce the uncertainty on  
209 the estimated stream parameters. On the evidence of high removal efficiencies observed by  
210 Böhlke and Denver (1995) we included stream scenarios ('Fixed CU') for which the confining  
211 unit removal efficiency was assumed to be perfectly known as 0.80. Similarly, it was assumed  
212 that the use of the TTD scaling parameters – while admitting a hydrologically realistic degree of  
213 flexibility to the simulated groundwater lag times – increased uncertainty on the estimates of  
214 stream removal rates. To query this effect we included an additional calibration scenario ('No  
215 TTD Scaling') for which the stream base-flow TTD simulated by the base model was fixed (**Table**  
216 **1**).

### 217 **3 RESULTS**

#### 218 **3.A Nitrate loading to the water table**

219 The calibrated loading scenarios collectively reproduce the relative mean groundwater  
220 nitrate concentration in each subcatchment as well as the preponderance of individual  
221 observed values (**Figure 4**), though some groundwater monitoring locations are not well-

222 simulated by any of the scenarios. Simulated values in the Morgan Creek catchment (e.g., at  
223 well KEBE206, labeled on **Figure 4**) are much more sensitive to the calibration structure than  
224 are simulated values in Chesterville Branch; this is expected given that simulated subsurface  
225 travel times in Morgan Creek are more sensitive to assumptions about the BFI than are those in  
226 Chesterville Branch (cf. Zell et al., 2018). For both subcatchments the mean simulated value is  
227 slightly lower than the mean observed value due to two features of the stage 1 regression  
228 methodology. First, all simulated and observed groundwater nitrate concentrations were  
229 transformed by the natural log in order to prevent the measurements of very high nitrate  
230 concentrations from dominating the regression. Second, observation variance was higher (and  
231 therefore observation weights were lower) for the highest concentrations.

232

**Insert Figure 4**

### 233 **3.B Catchment nitrate controls**

234 For stage 2 of parameter estimation each stream nitrate model was driven by a different  
235 nitrate loading scenario but calibrated against an identically weighted dataset of stream nitrate  
236 observations; therefore, unlike calibration stage 1, the weighted sum of square errors (WSSE)  
237 provides a comparative measure of stream model performance (**Figure 5**). The models  
238 collectively show that stream processes in Morgan Creek remove a higher fraction of incoming  
239 loads (0.55-0.77) than do stream processes in Chesterville Branch (0.05-0.41); for the nine best  
240 performing models, the range of calibrated removal rates for Chesterville Branch is even lower  
241 (0.05-0.19), though for most cases the estimate for Chesterville Branch is highly uncertain. The  
242 large uncertainty bounds for the Chesterville Branch removal parameter reflect the relatively

243 large measurement variability for the Chesterville Branch base-flow nitrate concentrations used  
244 as calibration targets (**Figure 6a**). As measured by the WSSE, nine of the twelve resulting  
245 calibration scenarios performed similarly (i.e., with calibration WSSE  $\leq 0.25$  of the highest  
246 WSSE) in their capacity to reproduce the stream nitrate time series (**Figure 5** and **Table 1**). With  
247 the exception of Loading Scenario B, each of the LowBFI models performed better than the  
248 corresponding HighBFI model; this performance difference may corroborate the results of the  
249 earlier calibration studies, which found that the LowBFI hydrology model performed better  
250 than the HighBFI hydrology model in its simulation of water levels and atmospheric tracer  
251 transport.

#### 252 **Insert Figure 5**

253 While the nitrate removal impact of the confining unit is well-demonstrated from the  
254 interpretation of individual wells in the Morgan Creek catchment (Böhlke and Denver, 1995),  
255 the catchment-level impact of the confining unit on nitrate removal is uncertain given the  
256 available data and the subsurface model used in this study (i.e., the simulated location of the  
257 confining unit and its resulting impact on the flow regime and nitrate removal). Assigning the  
258 confining unit a very high removal rate (i.e., the Fixed CU scenario) did result in the lowest  
259 estimate of in-stream/near-stream removal rates but did not meaningfully impact the model  
260 performance or the uncertainty associated with the remaining estimated parameters. In  
261 contrast, removing the TTD scaling parameters did greatly reduce the uncertainty of the  
262 estimated removal rates for both Chesterville Branch stream processing and the confining unit  
263 but at the cost of model performance.



285 those derived from the base-model calibration against subsurface tracer data (**Figure S3**); the  
286 calibrated shift is greater for Morgan Creek and results in a median age older than the median  
287 age in Chesterville Branch. As other authors have discussed (cf. Kirchner, 2006) parameters  
288 used to describe environmental systems may function as proxies for processes that are not  
289 explicitly represented in a model. In this case, in-stream nitrate data may be informing the  
290 base-flow TTD previously constrained by the subsurface tracer data; however, it is also possible  
291 that the calibrated TTD scaling factors reflect other hydrological or geochemical dynamics that  
292 would likewise delay the translation of the fertilizer purchase record to an in-stream water  
293 quality signal. For example, any subsurface retardation of nitrate relative to the non-retarded  
294 transport of atmospheric tracers would, under our conceptual model, be subsumed by  
295 adjustments to the TTD; these velocity differences could result from nitrate sorption, which is  
296 generally considered to be negligible but has been observed in some column studies (Clay et al.,  
297 2004). Similarly, TTD adjustments here could be in response to dispersive effects not evident  
298 during base model calibration nor represented by our advective assumptions....

#### 299 **4 DISCUSSION AND CONCLUSIONS**

300 Quantifying background controls on nitrate transport and removal is essential for their  
301 subsequent disentanglement from water quality trends that may be due to management  
302 actions. As such, this study provides a baseline characterization of nitrate transport timescales  
303 and removal mechanisms that will support future efforts to detect water quality benefits from  
304 ongoing BMP implementation. Simulated groundwater nitrate concentrations for several sites  
305 were highly sensitive to the range of stage 1 calibration scenarios (**Figure 4**). The poorly

306 performing groundwater sites are likely a result of local heterogeneity of either the flow system  
307 or the nitrate loading at a spatial scale not available to our discretization. For example,  
308 groundwater nitrate measurements include observations from three closely-spaced transects of  
309 3-4 wells each that sampled shallow groundwater in the lower reach of Morgan Creek (these  
310 include wells KEBD162 and KEBD163 – cf. **Figure 4**). This small area (i.e., all observations  
311 separated by less than 300 meters) is subject to very steep nitrate gradients that cannot be  
312 reproduced by our catchment-scale model. These gradients appear to be due to a combination  
313 of converging flow paths of widely disparate ages, nitrate removal due to denitrification in the  
314 confining unit sediments, and concentrated near-stream loading that possibly originates at a  
315 dairy operation near lower Morgan Creek (Puckett et al., 2008; Bachman et al., 2002; Böhlke  
316 and Denver, 1995).

317 While the sensitivity of simulated groundwater nitrate to the range of stage 1 calibration  
318 scenarios may suggest the importance of multiple plausible estimates of water table loading,  
319 the loading time series derived directly from the county-scale agricultural nitrate budget,  
320 without subsequent conditioning on groundwater nitrate data, resulted in similar calibrated  
321 stream models (**Figure 5**). Thus, for purposes of estimating long-term catchment nitrate  
322 controls from annually averaged stream nitrate concentrations, the available groundwater  
323 nitrate data did not substantially affect either the estimate of total nitrate available for stream  
324 export or the distribution of those inputs across the landscape. However, upland groundwater  
325 nitrate data and the specification of spatially distributed inputs may be more important for  
326 resolving nitrate export behavior at shorter timescales or when using a transient flow and



327 transport simulation to characterize subsurface linkages. For example, several studies have  
328 shown that in-stream nitrate concentrations can be highly sensitive to the time-variable  
329 hydrological connectivity that delivers base-flow from uplands to discharge areas (Petry et al.,  
330 2002; Ocampo et al., 2006; Wriedt et al., 2006; Molenat et al., 2008). The wide sub-annual  
331 range of base-flow nitrate concentrations shown in **Figure 6a** may reflect seasonal changes in  
332 upland gradients and leachate flushing as more permeable upland or midslope areas are  
333 activated and deactivated with rising and falling water tables. These effects, as well as the  
334 temperature-dependent stream metabolism effects on nitrogen removal (Bernot et al., 2006),  
335 are not captured by our simulation of the long-term export signal.

336 The current analysis cannot conclusively explain the disparate removal rates between the  
337 two catchments. However, two potential factors may be considered. Studies in the last decade  
338 (Wollheim et al., 2006, Mulholland et al., 2008; Alexander et al., 2009; Böhlke et al., 2009;  
339 Scanlon et al., 2010) have variously shown nitrate removal efficiency in smaller order streams  
340 to be a function of hydraulics (i.e., stream depth or velocity) or water quality (i.e., stream  
341 nitrate concentration). At shallow depths and low velocities, stream nitrates have longer  
342 exposure to nitrogen uptake services from in-channel biota and sediments (Alexander et al.,  
343 2009). Near-stream and in-stream hydraulics are likely of importance here; i.e., as described  
344 above, the confining unit which outcrops in the Morgan Creek lower reaches may not only  
345 account for nitrogen removal through denitrification, but also controls the seepage of base-  
346 flow discharge to the main channel in a manner that increases exposure of nitrates to biotic  
347 uptake. Furthermore, a coarse comparison of the stream velocities and associated cross-

348 sectional flow areas (**Figure S3**) suggests that Chesterville Branch has shorter in-stream  
349 residence times due to a shorter network and higher velocities. The National Hydrography  
350 Dataset (NHDPlusV2) approximation of the Morgan Creek stream network (above the gage  
351 used in this study) is approximately 3.5 times the length of Chesterville Branch (also above the  
352 gage), such that the length-normalized removal efficiencies may be more similar than their  
353 accumulated downstream effect.

354 Less well understood is the evidence that nitrogen removal efficiency declines with  
355 increasing nitrate concentration. For example, Mulholland et al. (2008) found across a range of  
356 smaller order streams that increasing the stream nitrate concentration from 1.5 to 15 mg/L  
357 may reduce the nitrate removal fraction by more than half. The results of this study may  
358 reiterate questions of potential importance for management of nitrogen export from lower  
359 order streams; namely, are the low removal rates in Chesterville Branch (i) a characteristic of  
360 the natural system or (ii) a legacy of stream degradation? If the latter, might nitrate processing  
361 be improved (i.e., restored) by reducing the headwater loads? Further study is required to  
362 evaluate the relative importance of headwater loads versus loads from tributaries or base-flow  
363 discharge further downstream at the subcatchment outlet (see **Figure S4**), and whether these  
364 loads are responsible for degrading the in-stream processing capacity. These future studies  
365 could include prediction uncertainty analysis and monitoring network design that would reduce  
366 the uncertainty associated with the relative influence of confining unit and in-stream/near-  
367 stream mechanisms. But the results of this analysis suggest a greater urgency for placement of

368 BMPs in the Chesterville Branch catchment as well as continued in-stream monitoring that may  
369 detect their potential effects.

## 370 **5 ACKNOWLEDGEMENTS**

371 This study received funding by the National Science Foundation under award numbers  
372 CBET-0846244 and CCF-1451708. The authors thank Jim Tesoriero and two anonymous  
373 reviewers for their improvements to the manuscript.

## 374 **6 DATA AVAILABILITY**

375 The data generated during this study, including input and output files for the simulations  
376 referred to in the manuscript, are available as a USGS data release (Zell and Sanford, 2019).

## 377 **7 SUPPLEMENTAL MATERIAL**

378 The supplemental material for this manuscript describes the model development and  
379 calibration procedure in greater detail.

380 **8 WORKS CITED**

381

382 Alexander, R. B., Böhlke, J. K., Boyer, E. W., David, M. B., Harvey, J. W., Mulholland, P. J.,  
383 Wollheim, W. M. (2009). Dynamic modeling of nitrogen losses in river networks unravels the  
384 coupled effects of hydrological and biogeochemical processes. *Biogeochemistry*, *93*(1-2), 91-  
385 116.

386

387 Aquilina, L., Vergnaud-Ayraud, V., Labasque, T., Bour, O., Molénat, J., Ruiz, L., ... &  
388 Longuevergne, L. (2012). Nitrate dynamics in agricultural catchments deduced from  
389 groundwater dating and long-term nitrate monitoring in surface-and groundwaters. *Science of*  
390 *the Total Environment*, *435*, 167-178.

391

392 Arnold, J. G., Allen, P. M., Muttiah, R., & Bernhardt, G. (1995). Automated base flow  
393 separation and recession analysis techniques. *Groundwater*, *33*(6), 1010-1018.

394

395 Ator, S. W., & Denver, J. M. (2012). Estimating contributions of nitrate and herbicides from  
396 groundwater to headwater streams, Northern Atlantic Coastal Plain, United States. *JAWRA*  
397 *Journal of the American Water Resources Association*, *48*(6), 1075-1090.

398

399 Bachman, L. J., Krantz, D. E., Böhlke, J., & Hantush, M. M. (2002). Hydrogeologic framework,  
400 ground-water geochemistry, and assessment of nitrogen yield from base flow in two  
401 agricultural watersheds, Kent County, Maryland. U.S. Environmental Protection Agency,  
402 Washington, D.C., EPA/600/R-02/008.

403

404 Bernot, M. J., Tank, J. L., Royer, T. V., & David, M. B. (2006). Nutrient uptake in streams  
405 draining agricultural catchments of the midwestern United States. *Freshwater Biology*, *51*(3),  
406 499-509.

407

408 Böhlke, J. K., & Denver, J. M. (1995). Combined use of groundwater dating, chemical, and  
409 isotopic analyses to resolve the history and fate of nitrate contamination in two agricultural  
410 watersheds, Atlantic Coastal Plain, Maryland. *Water Resources Research*, *31*(9), 2319-2339.

411

412 Böhlke, J. K., Antweiler, R. C., Harvey, J. W., Laursen, A. E., Smith, L. K., Smith, R. L., &  
413 Voytek, M. A. (2009). Multi-scale measurements and modeling of denitrification in streams with  
414 varying flow and nitrate concentration in the Upper Mississippi River Basin, USA.  
415 *Biogeochemistry*, *93*(1-2), 117-141.

416

417 Boyer, E. W., Alexander, R. B., Parton, W. J., Li, C., Butterbach-Bahl, K., Donner, S. D., ... &  
418 Grosso, S. J. D. (2006). Modeling denitrification in terrestrial and aquatic ecosystems at regional  
419 scales. *Ecological Applications*, *16*(6), 2123-2142.

420

421 Clay, D. E., Zheng, Z., Liu, Z., Clay, S. A., & Trooien, T. P. (2004). Bromide and nitrate  
422 movement through undisturbed soil columns. *Journal of Environmental Quality*, 33(1), 338-342.

423

424 Clune, J. W., & Denver, J. M. (2012). *Residence time, chemical and isotopic analysis of*  
425 *nitrate in the groundwater and surface water of a small agricultural watershed in the coastal*  
426 *plain, Bucks Branch, Sussex County, Delaware*. U.S. Geological Survey Scientific Investigations  
427 Report 2012-5235.

428

429 Conan, C., Bouraoui, F., Turpin, N., de Marsily, G., & Bidoglio, G. (2003). Modeling flow and  
430 nitrate fate at catchment scale in Brittany (France). *Journal of Environmental Quality*, 32(6),  
431 2026-2032.

432

433 Duff, J. H., Tesoriero, A. J., Richardson, W. B., Strauss, E. A., & Munn, M. D. (2008). Whole-  
434 stream response to nitrate loading in three streams draining agricultural landscapes. *Journal of*  
435 *Environmental Quality*, 37(3), 1133-44.

436

437 Fienen, M. N., Muffels, C. T., & Hunt, R. J. (2009). On constraining pilot point calibration  
438 with regularization in PEST. *Groundwater*, 47(6), 835-844.

439

440 Galbiati, L., Bouraoui, F., Elorza, F. J., & Bidoglio, G. (2006). Modeling diffuse pollution  
441 loading into a Mediterranean lagoon: development and application of an integrated surface-  
442 subsurface model tool. *Ecological Modelling*, 193(1-2), 4-18.

443

444 Gitau, M. W., Chaubey, I., Gbur, E., Pennington, J. H., & Gorham, B. (2010). Impacts of land-  
445 use change and best management practice implementation in a conservation effects  
446 assessment project watershed: Northwest Arkansas. *Journal of Soil and Water Conservation*,  
447 65(6), 353-368.

448

449 Green, C. T., Puckett, L. J., Böhlke, J. K., Bekins, B. A., Phillips, S. P., Kauffman, L. J., Denver,  
450 J.M., Johnson, H. M. (2008). Limited occurrence of denitrification in four shallow aquifers in  
451 agricultural areas of the United States. *Journal of Environmental Quality*, 37(3), 994-1009.

452

453 Harbaugh, A. W. (2005). MODFLOW-2005, the US geological survey modular ground-water  
454 model: The ground-water flow process. U.S. Geological Survey Techniques and Methods 6-A16.

455

456 Kirchner, J. W. (2006). Getting the right answers for the right reasons: Linking  
457 measurements, analyses, and models to advance the science of hydrology. *Water Resources*  
458 *Research*, 42(3).

459

460 Lindsey, B. D., Phillips, S. W., Donnelly, C. A., Speiran, G. K., Plummer, L. N., Böhlke, J.K.,  
461 Busenberg, E. (2003). Residence times and nitrate transport in ground water discharging to

462 streams in the Chesapeake Bay Watershed. U.S. Geological Survey Water-Resources  
463 Investigations Report 2003–4035.

464

465 Meals, D. W., Dressing, S. A., & Davenport, T. E. (2010). Lag time in water quality response  
466 to best management practices: A review. *Journal of Environmental Quality*, 39(1), 85-96.

467

468 Molénat, J., Gascuel-Oudou, C., Ruiz, L., & Gruau, G. (2008). Role of water table dynamics on  
469 stream nitrate export and concentration in agricultural headwater catchment (France). *Journal*  
470 *of Hydrology*, 348(3-4), 363-378.

471

472 Montreuil, O., Merot, P., & Marmonier, P. (2010). Estimation of nitrate removal by riparian  
473 wetlands and streams in agricultural catchments: effect of discharge and stream  
474 order. *Freshwater Biology*, 55(11), 2305-2318.

475

476 Mulholland, P. J., Helton, A. M., Poole, G. C., Hall, R. O., Hamilton, S. K., Peterson, B. J.,  
477 Dahm, C. N. (2008). Stream denitrification across biomes and its response to anthropogenic  
478 nitrate loading. *Nature*, 452(7184), 202-205.

479

480 Nelson, J., & Spies, P. (2013). The Upper Chester river watershed: Lessons learned from a  
481 focused, highly partnered, voluntary approach to conservation. *Journal of Soil and Water*  
482 *Conservation*, 68(2), 41A-44A.

483

484 Ocampo, C. J., Sivapalan, M., & Oldham, C. (2006). Hydrological connectivity of upland-  
485 riparian zones in agricultural catchments: Implications for runoff generation and nitrate  
486 transport. *Journal of Hydrology*, 331(3-4), 643-658.

487

488 Osmond, D., Meals, D., Hoag, D., Arabi, M., Luloff, A., Jennings, G., Line, D. (2012).  
489 Improving conservation practices programming to protect water quality in agricultural  
490 watersheds: Lessons learned from the National Institute of Food and Agriculture-Conservation  
491 Effects Assessment Project. *Journal of Soil and Water Conservation*, 67(5), 122A-127A.

492

493 Petry, J., Soulsby, C., Malcolm, I. A., & Youngson, A. F. (2002). Hydrological controls on  
494 nutrient concentrations and fluxes in agricultural catchments. *Science of the Total*  
495 *Environment*, 294(1-3), 95-110.

496

497 Pollock, D. W. (2012). User guide for MODPATH version 6: A particle tracking model for  
498 MODFLOW. U.S. Geological Survey Techniques and Methods 6-A41.

499

500 Puckett, L. J., Tesoriero, A. J., & Dubrovsky, N. M. (2011). Nitrogen contamination of surficial  
501 aquifers: A growing legacy. *Environmental Science and Technology*, 45(3), 839.

502

503 Puckett, L. J., Zamora, C., Essaid, H., Wilson, J. T., Johnson, H. M., Brayton, M. J., & Vogel, J.  
504 R. (2008). Transport and fate of nitrate at the ground-water/surface-water interface. *Journal of*  
505 *Environmental Quality*, 37(3), 1034-50.

506  
507 Royer, T. V., Tank, J. L., & David, M. B. (2004). Transport and fate of nitrate in headwater  
508 agricultural streams in Illinois. *Journal of Environmental Quality*, 33(4), 1296-1304.

509  
510 Sanford, W. E., & Pope, J. P. (2013). Quantifying groundwater's role in delaying  
511 improvements to Chesapeake Bay water quality. *Environmental Science and Technology*,  
512 47(23), 13330-13338.

513  
514 Scanlon, T. M., Ingram, S. M., & Riscassi, A. L. (2010). Terrestrial and in-stream influences on  
515 the spatial variability of nitrate in a forested headwater catchment. *Journal of Geophysical*  
516 *Research: Biogeosciences*, 115(G2).

517  
518 Schindler, D. W., & Vallentyne, J. R. (2008). *The Algal Bowl*. University of Alberta Press.

519  
520 Science and Technical Advisory Committee (2005). *Understanding Lag Times Affecting the*  
521 *Improvement of Water Quality in the Chesapeake Bay: A Report from the Chesapeake Bay*  
522 *Program Scientific and Technical Advisory Committee*. Science and Technical Advisory  
523 Committee Publication 5-001. Accessed August 8, 2019 at  
524 <http://www.chesapeake.org/pubs/lagtimereport.pdf>.

525  
526 Soil Survey Staff, Natural Resources Conservation Service, United States Department of  
527 Agriculture. Soil Survey Geographic (SSURGO) Database. Available online at  
528 <http://sdmdataaccess.nrcs.usda.gov/>.

529  
530 Staver, K. W., & Brinsfield, R. B. (1998). Using cereal grain winter cover crops to reduce  
531 groundwater nitrate contamination in the Mid-Atlantic Coastal Plain. *Journal of Soil and Water*  
532 *Conservation*, 53(3), 230-240.

533  
534 Sutton, A. J., Fisher, T. R., & Gustafson, A. B. (2009). Historical changes in water quality at  
535 German Branch in the Choptank River Basin. *Water, Air, & Soil Pollution*, 199(1), 353-369.

536  
537 Tesoriero, A.J., Duff, J.H., Saad, D.A., Spahr, N.E. and Wolock, D.M., 2013. Vulnerability of  
538 streams to legacy nitrate sources. *Environmental Science and Technology*, v. 47, 3623-3629.

539  
540 U.S. Geological Survey, 2016, USGS water data for the Nation: U.S. Geological Survey  
541 National Water Information System database, accessed January 29, 2016,  
542 at <https://doi.org/10.5066/F7P55KJN>.

543

- 544 Wei, X., Bailey, R. T., Records, R. M., Wible, T. C., & Arabi, M. (2018). Comprehensive  
545 simulation of nitrate transport in coupled surface-subsurface hydrologic systems using the  
546 linked SWAT-MODFLOW-RT3D model. *Environmental Modelling & Software*.  
547
- 548 Wollheim, W. M., Vörösmarty, C. J., Peterson, B. J., Seitzinger, S. P., & Hopkinson, C. S.  
549 (2006). Relationship between river size and nutrient removal. *Geophysical Research Letters*,  
550 33(6).  
551
- 552 Wriedt, G., Spindler, J., Neef, T., Meißner, R., & Rode, M. (2007). Groundwater dynamics  
553 and channel activity as major controls of in-stream nitrate concentrations in a lowland  
554 catchment system? *Journal of Hydrology*, 343(3-4), 154-168.  
555
- 556 Vidon, P. G., & Hill, A. R. (2004). Landscape controls on nitrate removal in stream riparian  
557 zones. *Water Resources Research*, 40(3).  
558
- 559 Vitousek, P. M., Aber, J. D., Howarth, R. W., Likens, G. E., Matson, P. A., Schindler, D. W.,  
560 Schlesinger, W.H., and Tilman, D. G. (1997). Human alteration of the global nitrogen cycle:  
561 sources and consequences. *Ecological Applications*, 7(3), 737-750.  
562
- 563 Yevenes, M. A., and Mannaerts, C. M. (2012). Untangling hydrological pathways and nitrate  
564 sources by chemical appraisal in a stream network of a reservoir catchment. *Hydrology and  
565 Earth System Sciences*, 16(3), 787-799.  
566
- 567 Zell, W. O., Culver, T. B., & Sanford, W. E. (2018). Prediction uncertainty and data worth  
568 assessment for groundwater transport times in an agricultural catchment. *Journal of  
569 Hydrology*, 561, 1019-1036.  
570
- 571 Zell, W.O., and Sanford, W.E. (2019). MODFLOW-2005 and MODPATH6 models used to  
572 simulate groundwater flow and nitrate transport in two tributaries to the Upper Chester River,  
573 Maryland. U.S. Geological Survey data release. <https://doi.org/10.5066/P9VWY11M>



574 **9 FIGURE CAPTIONS**

575 **Figure 1.** Upper Chester study area. The heavy black line delineates the model domain.

576

577 **Figure 2.** (a) Crop acreage, (b) agricultural nitrogen inputs and exports, and (c) estimated nitrate concentrations  
578 for agricultural recharge in Kent County, MD. See the Supplemental Materials for a complete description of the  
579 input and export datasets and the calculation of the recharging nitrate time series. The high loading scenario is the  
580 rate calculated by restricting the county-scale mass of recharging nitrate to only reported corn acreage, as  
581 implemented in Equation S3 and used in this study. The low loading scenario is the rate calculated by distributing  
582 the recharging nitrate load to the sum of reported corn, soybean and wheat acreage and shown here only for  
583 purposes of comparison.

584

585 **Figure 3.** Observed stream nitrate concentrations at the (a) Morgan Creek and (b) Chesterville Branch gages (see  
586 **Figure 1** for gage locations). Crosses show those observations determined to have occurred under base-flow  
587 conditions and used to formulate calibration targets for this study; hollow circles show observations determined to  
588 have occurred under event flow conditions. See Figure 6 for time periods of data collection. Stream discharge and  
589 nitrate concentrations downloaded from the National Water Information System (NWIS; U.S. Geological Survey,  
590 2016).

591

592 **Figure 4. Simulated vs. observed groundwater nitrate concentrations** for (a) upland and (b) riparian locations for  
593 the spatially-distributed nitrate loading scenarios estimated during stage 1 of model calibration. Each vertical line  
594 shows the range of nitrate values simulated by the multiple calibration scenarios for a single point in space and  
595 time (recalling that some observation locations have multiple measurements).

596

597 **Figure 5.** Model performance and estimated values for nitrate removal parameters for the Stage 2 calibration  
598 scenarios. The 'Fixed CU' and 'No TTD Scaling' scenarios are described in the text; see the Supplemental Material

599 for full description of the remaining scenarios. Error bars express +/- two standard deviations, calculated by PEST++  
600 using Schur's complement (cf. Fienen et al., 2010).

601

602 **Figure 6. Simulated stream nitrate.** The shading in (a) shows the range of concentrations simulated by the nine  
603 models with the lowest WSSE (see **Table 1**); markers in (a) show the annually-averaged stream concentrations  
604 used as calibration targets; the error bars for each marker show the range of base-flow nitrate concentrations from  
605 which the annual average was calculated. Error bars without an accompanying marker show data acquired after  
606 model development and not used in calibration. The shaded and hatched regions in (b) are computed from the  
607 mean of the nine models with the lowest WSSE (see **Figure 5**); the dashed line in (b) show the simulated results of  
608 the single Fixed CU scenario.

## 609 10 TABLES

**Table 1. Model Scenarios.** WSSE = Weighted sum of squared errors calculated during stream model calibration. Model performance rank is 1 (best) to 12 (worst) and is discussed in the Results section, below.

Stage 1: Nitrate Loading to Water Table			Stage 2: Nitrate Removal		
Base Model	Loading Scenario Name	Groundwater NO <sub>3</sub> Weighting Scheme	Stream Scenario Name	Fixed Parameters	Model Rank (WSSE)
Low BFI	LowBFI Reference	[No additional calibration; spatially-constant loading derived from county data]	LowBFI Reference		3 (138)
	LowBFI A	Standard error of measurement	LowBFI A		1 (116)
	LowBFI B	Natural log of standard error of measurement	LowBFI B		12 (1225)
	LowBFI Mean	[No additional calibration; each pixel in the loading field equal to the mean of the A and B scenarios]	LowBFI Mean		2 (120)
			LowBFI FixedCU	Confining Unit Removal Fraction = 0.80	4 (172)
			LowBFI No TTD Scaling	TTD Scale Factor = 1	10 (482)
High BFI	HighBFI Reference	[No additional calibration; spatially-constant loading derived from county data]	HighBFI Reference		8 (257)
	HighBFI A	Standard error of measurement	HighBFI A		5 (190)
	HighBFI B	Natural log of standard error of measurement	HighBFI B		7 (234)
	HighBFI Mean	[No additional calibration; each pixel in the loading field equal to the mean of the A and B scenarios]	HighBFI Mean		6 (197)
			HighBFI FixedCU	Confining Unit Removal Fraction = 0.80	9 (302)
			HighBFI No TTD Scaling	TTD Scale Factor = 1	11 (901)

610

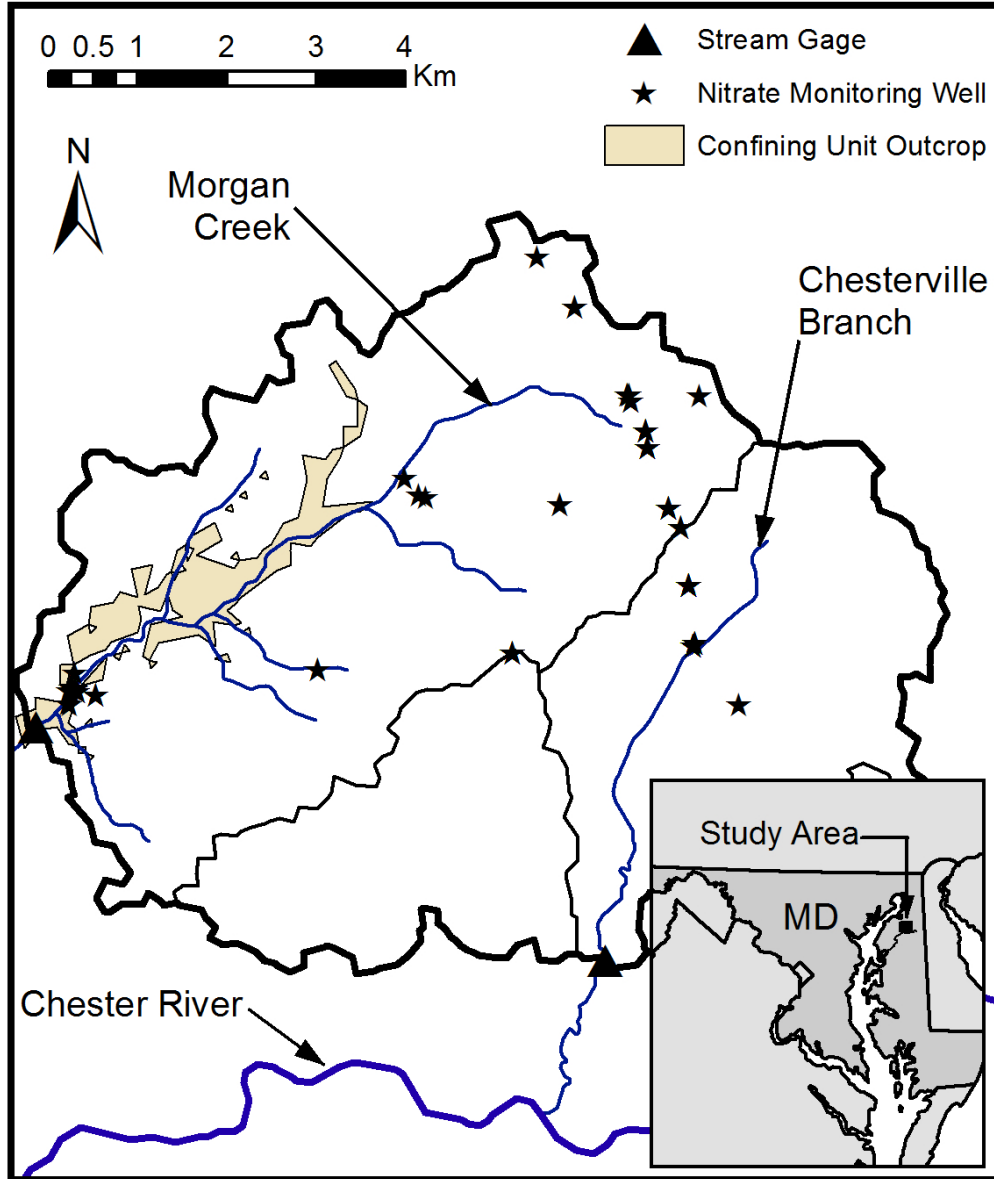


Figure 1. Upper Chester study area. The heavy black line delineates the model domain.

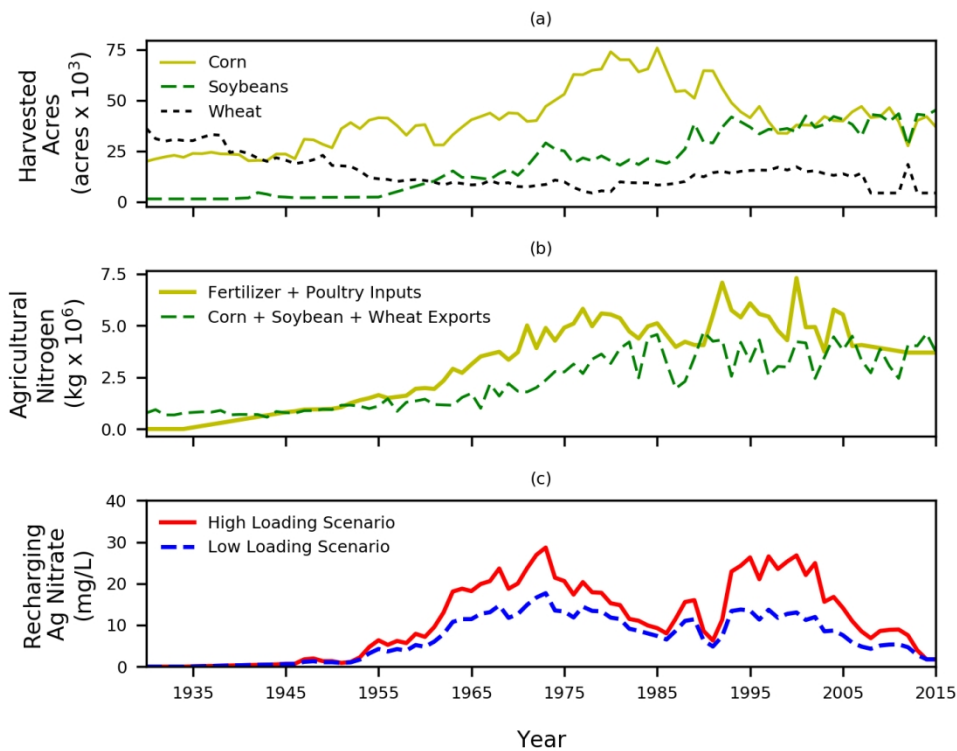


Figure 2. (a) Crop acreage, (b) agricultural nitrogen inputs and exports, and (c) estimated nitrate concentrations for agricultural recharge in Kent County, MD. See the Supplemental Materials for a complete description of the input and export datasets and the calculation of the recharging nitrate time series. The high loading scenario is the rate calculated by restricting the county-scale mass of recharging nitrate to only reported corn acreage, as implemented in Equation S3 and used in this study. The low loading scenario is the rate calculated by distributing the recharging nitrate load to the sum of reported corn, soybean and wheat acreage and shown here only for purposes of comparison.

127x101mm (300 x 300 DPI)

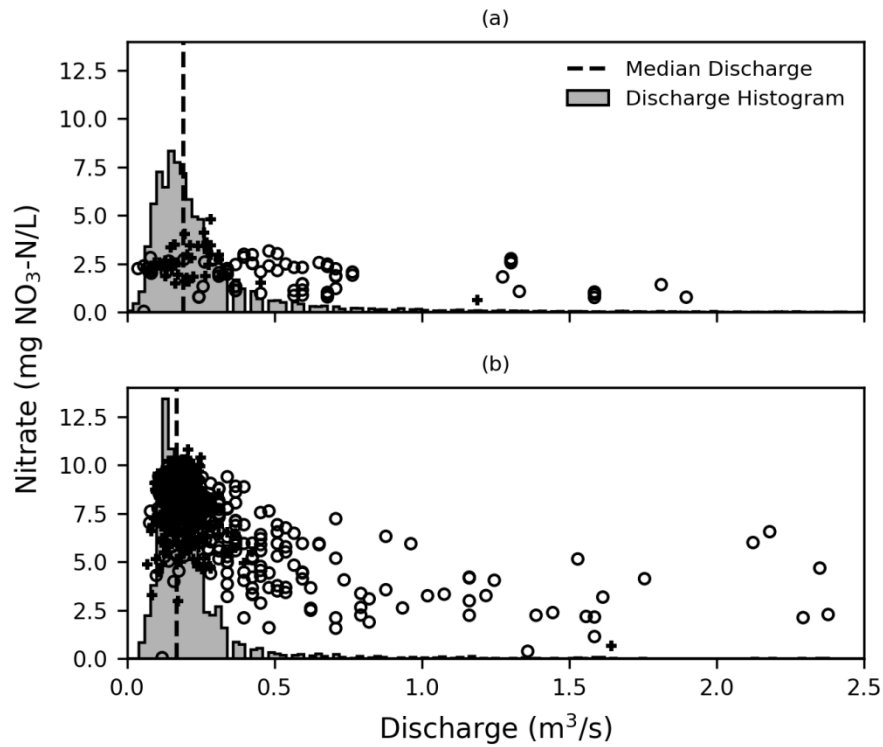


Figure 3. Observed stream nitrate concentrations at the (a) Morgan Creek and (b) Chesterville Branch gages (see Figure 1 for gage locations). Crosses show those observations determined to have occurred under base-flow conditions and used to formulate calibration targets for this study; hollow circles show observations determined to have occurred under event flow conditions. See Figure 6 for time periods of data collection. Stream discharge and nitrate concentrations downloaded from the National Water Information System (NWIS; U.S. Geological Survey, 2016).

127x101mm (300 x 300 DPI)

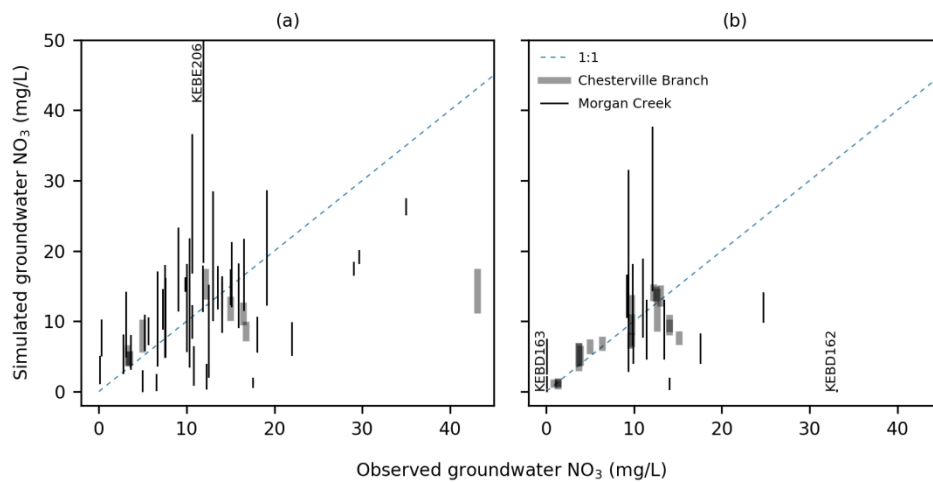


Figure 4. Simulated vs. observed groundwater nitrate concentrations for (a) upland and (b) riparian locations for the spatially-distributed nitrate loading scenarios estimated during stage 1 of model calibration. Each vertical line shows the range of nitrate values simulated by the multiple calibration scenarios for a single point in space and time (recalling that some observation locations have multiple measurements).

158x88mm (300 x 300 DPI)

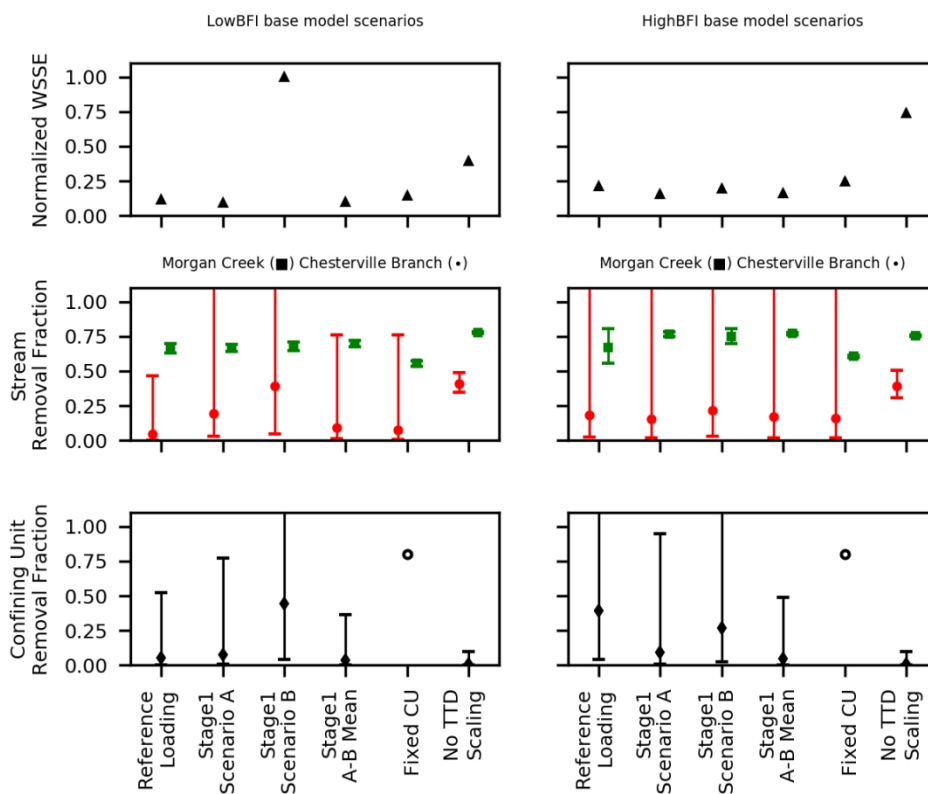


Figure 5. Model performance and estimated values for nitrate removal parameters for the Stage 2 calibration scenarios. The 'Fixed CU' and 'No TTD Scaling' scenarios are described in the text; see the Supplemental Material for full description of the remaining scenarios. Error bars express +/- two standard deviations, calculated by PEST++ using Schur's complement (cf. Fienen et al., 2010).

107x88mm (300 x 300 DPI)



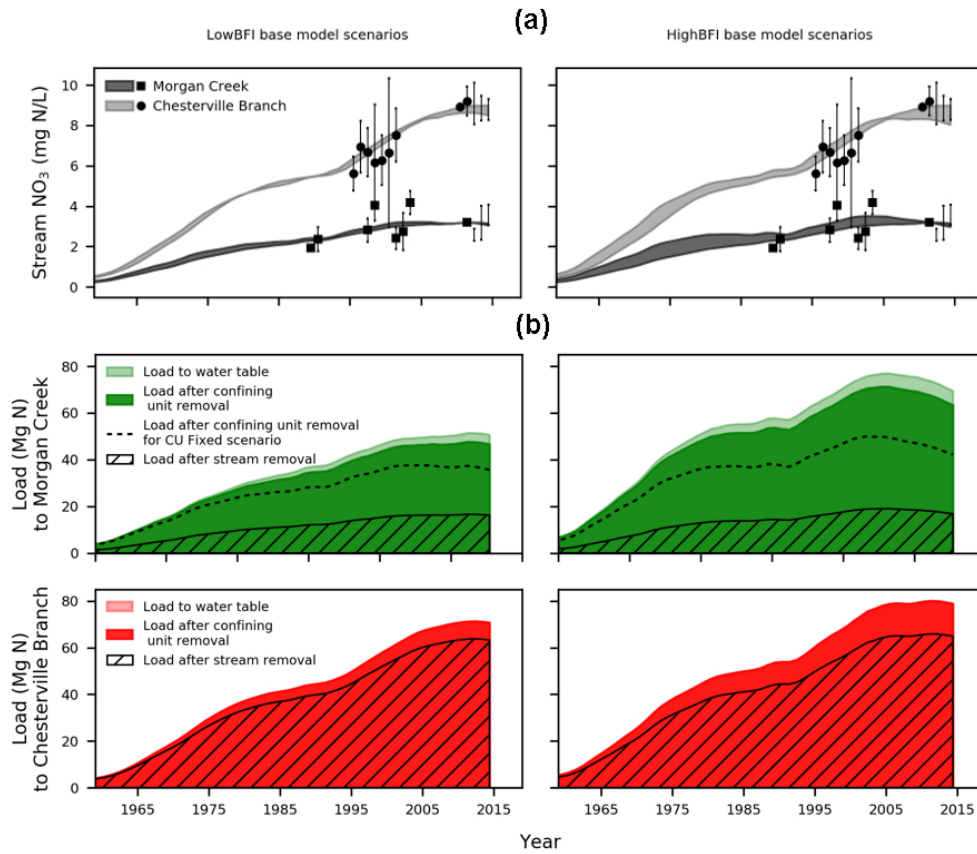


Figure 6. Simulated stream nitrate. The shading in (a) shows the range of concentrations simulated by the nine models with the lowest WSSE (see Table 1); markers in (a) show the annually-averaged stream concentrations used as calibration targets; the error bars for each marker show the range of base-flow nitrate concentrations from which the annual average was calculated. Error bars without an accompanying marker show data acquired after model development and not used in calibration. The shaded and hatched regions in (b) are computed from the mean of the nine models with the lowest WSSE (see Figure 5); the dashed line in (b) show the simulated results of the single Fixed CU scenario.

158x135mm (144 x 144 DPI)

**Supplemental Materials for:**

**Quantifying Background Nitrate Removal Mechanisms in an Agricultural Watershed with Contrasting Subcatchment Base-flow Concentrations**

Wesley O. Zell<sup>1</sup> (wzell@usgs.gov) \*corresponding author

Teresa B. Culver<sup>2</sup> (tbc4e@virginia.edu)

Ward E. Sanford<sup>1</sup> (wsanford@usgs.gov)

Jonathan L. Goodall<sup>2</sup> (goodall@virginia.edu)

<sup>1</sup> U.S. Geological Survey, 12201 Sunrise Valley Dr, MS 432, Reston, VA 20192

<sup>2</sup> Department of Civil and Environmental Engineering, University of Virginia, Thornton Hall, P.O. Box 400259, Charlottesville, VA 22904-4259

**This supplemental materials section contains 20 pages, including 3 tables and 5 figures.**

## **S1 CALCULATION OF NITRATE INPUTS TO THE WATER TABLE**

### **S1.A Estimation of nitrate loading to the water table in monitored portions of the catchment (Calibration Stage 1a)**

Nitrate loading to the water table was first estimated by calibrating the nitrate transport model solely against observed groundwater nitrate concentrations. Groundwater nitrate observations were downloaded from the U.S. Geological Survey (USGS) National Water Information System (NWIS; U.S. Geological Survey, 2016) and aggregated into annually averaged concentrations at each observation well; in total, 213 subsurface nitrate measurements at 52 different wells were aggregated into 89 subsurface calibration targets that date between 1988 and 2004 (see **Figure 1** in manuscript for locations of nitrate monitoring wells).

In order to allow spatial variation of water table nitrate loading, we parameterized the inputs as a two-dimensional (2D) set of loading factors. Loading factors were estimated using an evenly spaced grid of pilot points, with pilot point separation approximating the length scale of the smallest agricultural fields. The 2D loading field of nitrate inputs was then interpolated from the loading factors using ordinary kriging implemented with the PEST utilities PPKFAC and FAC2REAL (Doherty, 2015). Parameter estimation was performed using PEST ++ (Welter et al., 2015) with singular value decomposition (SVD) and preferred-value Tikhonov regularization. Briefly stated, these regularization devices make a highly parameterized inverse-modeling problem well-posed and avoid over-fitting by constraining a parameter value to some prior estimate unless the calibration data provide a compelling reason for that estimate to change; cf. Fienen et al. (2009) for more detailed description of this parameter estimation methodology.

For the years 1930-2015, spatially and temporarily variable nitrate inputs were calculated by multiplying the interpolated loading factors by a reference load derived from agricultural and wet deposition components for that year; agricultural loading prior to 1930 was assumed to be zero. The reference load for each year consisted of an agricultural portion and a wet deposition portion. The agricultural portion of the reference load for each year was derived from county-level nitrogen budgets, with the total mass of agricultural nitrogen available for recharge in year  $i$  calculated as

$$N_{tot,in,i} = N_{ag,in,i} - N_{ag,out,i} \quad \text{(Eq. S1)}$$

where  $N_{ag,in}$  is the agricultural nitrogen inputs and  $N_{ag,out}$  is the agricultural nitrogen exports. Historical county-level agricultural nitrogen inputs were derived from estimated and reported inorganic fertilizer sales (Alexander and Smith, 1990; Gronberg and Spahr, 2012; Brakebill and Gronberg, 2017) and estimates of poultry manure production (Sanford and Pope, 2013) (see **Figure 3** in manuscript). Historical county-level agricultural nitrogen exports were derived from the annual production of corn, soybeans, and wheat as published by the National Agricultural Statistics Service (NASS). The amount produced of each crop was converted to mass nitrogen by assuming the nitrogen content of harvested crops to be 0.9, 3.8, and 1.5 pounds nitrogen per bushel for corn, soybeans, and wheat, respectively (Murrell, 2008). In the Mid-Atlantic as much as 65-75% of the nitrogen content of soybeans can be due to atmospheric fixation and not to fertilizer inputs (<http://extension.udel.edu/factsheets/nitrogen-management-for-soybean>); for our mass balance calculations we consequently adjusted the nitrogen content coefficient of soybeans to 1.1 pounds nitrogen exported per bushel. The nitrogen within

reported harvested silage (which is not reported for the full period of record) was assumed to remain in the catchment and thus be available for leaching.

For each year, county-level estimates of the residual nitrogen available after crop uptake (Eq. 2) were converted to an areal loading rate that was applied within the model domain. Corn receives a much higher fraction of total fertilizer inputs for a given year than other crops (Hancock and Brayton, 2006), such that the ratio of fertilizer sales to harvested corn acreage provides a provisional estimate of the areal loading rate for those areas where it was applied. We consequently calculated the reference rate for year  $i$  as

$$Rate_{Ref,i} = \frac{N_{tot,in,i}}{Area\ Corn_i} + Rate_{atm,i} \quad (\text{Eq. S2})$$

where  $N_{tot,in,i}$  is the county-level mass of nitrogen remaining after crop export for year  $i$  (Eq. S1),  $Area\ Corn_i$  is the county-level area of harvested corn for the year  $i$ , and  $Rate_{atm,i}$  is rate of annual wet deposition. Rates of nitrate wet deposition were obtained from the National Atmospheric Deposition Program monitoring site in Wye, Maryland, approximately 30 miles southeast of the study site (data downloaded from <http://nadp.sws.uiuc.edu> on 6/4/2015). Wet deposition data were available from 1983-2006. We assumed zero wet deposition for years prior to 1935; for years between 1935 and 1983 we used a linear interpolation to estimate annual wet deposition rates.

Several factors govern the delivery of excess nitrates to the water table and their transport through the subsurface to discharge locations. For example, multiple researchers have shown the particular sensitivity of leachate concentrations to precipitation patterns, as rainfall deficits during the growing season reduce crop uptake efficiencies and increase pools of excess nitrate

(Burt et al., 2008), while large rainfall amounts post-harvest accelerate nitrate flushing from the root zone to the water table (Staver and Brinsfield, 1998). In order to account for the dampening of the nitrate input signal that likely occurs at a given location through delays and mixing in the root zone and unsaturated zone (as well as similar dampening that would occur due to crop rotation – cf. Hancock and Brayton, 2006), we transformed the time series calculated with **Equation S2** using a 3-year moving average.

Note that in the case of an input signal that is constant across the landscape at a given time (as is effectively true, e.g., of age tracers that recharge from the atmosphere), the contributing recharge area for each monitoring location is unimportant. However, even in a majority agricultural catchment, the sources of nitrate may vary dramatically across the landscape, such that for purposes of simulating the nitrate concentration at monitoring wells the input signal must be specified with respect to both time and space. We generated distinct estimated distributions of loading factors by performing the Stage 1 calibration with both the LowBFI and HighBFI transport base models. In addition, we used two different weighting schemes to determine the relative importance of the different groundwater nitrate calibration targets during the optimization. Briefly stated, the weight for each annually averaged groundwater nitrate observation was initially calculated from the standard error of measurement (weighting scenario A) for all measurements within a given year (i.e., for the distribution of measurements that were aggregated into the annual average). Because this weighting scheme resulted in a large disparity of weights and a relatively small number of observations dominating the regression we also considered an alternative weighting scheme in which we reduced the range

of weights by using a natural log transform and enforcing a minimum weight (weighting scenario B). We therefore generated four separate water table loading scenarios for the monitored portion of the catchment. After extrapolation of the loading field from the monitored to the unmonitored portions of the catchment we generated additional loading scenarios by calculating – for each base model – the spatially distributed means of the two weighting scenarios (**Table S1**).

**Table S1.** Water table loading scenarios generated from Stage 1 of parameter estimation.

<u>Scenario Name</u>	<u>Base Model</u>	<u>Groundwater NO<sub>3</sub> Weighting Scheme</u>	<u>Additional Transformations</u>
<b>LowBFI Scenario A</b>	LowBFI	Standard error of measurement	--
<b>LowBFI Scenario B</b>	LowBFI	Natural log of scenario A weights	--
<b>LowBFI Scenario A-B Mean</b>	LowBFI	--	Spatially distributed field with each point equal to the mean of Distributed_A and Distributed_B scenarios
<b>HighBFI Scenario A</b>	HighBFI	Standard error of measurement	--
<b>HighBFI Scenario B</b>	HighBFI	Natural log of scenario A weights	--
<b>HighBFI Scenario A-B Mean</b>	HighBFI	--	Spatially distributed field with each point equal to the mean of A and B scenarios

### **S1.B Extrapolation of the estimated water table loading from the monitored portion to the unmonitored portions of the catchment (Calibration Stage 1b)**

Following the Stage 1a estimation of nitrate loading factors we differentiated (i) the portions of the estimated loading field that were well-constrained by the groundwater data from (ii) those portions that were not well-constrained and thus required some other mechanism for estimating the loading factor. We defined the 'monitored' portion of the landscape as those areas for which the post-calibration reduction in parameter uncertainty (i.e., compared to the pre-calibration parameter uncertainty) for the nitrate loading factor was at



least 10%, where the post-calibration parameter uncertainty is derived via linearized Bayesian methods,

$$\Sigma_{\theta,post} = \Sigma_{\theta} - \Sigma_{\theta} J^T [J \Sigma_{\theta} J^T + \Sigma_{\varepsilon}]^{-1} J \Sigma_{\theta} \quad (\text{Eq. S3})$$

where  $\Sigma_{\theta,post}$  is the post-calibration parameter covariance,  $\Sigma_{\theta}$  is the covariance matrix of prior parameter probability distribution (here derived from the estimated bounds on parameter values);  $J$  is the Jacobian matrix of observation sensitivity to parameter perturbations; and  $\Sigma_{\varepsilon}$  is the covariance matrix of simulation error and measurement error. For this study  $\Sigma_{\varepsilon}$  is defined as a diagonal matrix populated by the inverse of observation weights (all off-diagonal elements are equal to 0).

In order to extrapolate the water table nitrate loading to the entire simulation domain, we used a Gradient Boosted Regression (GBR; implemented with the Python scikit-learn library: Pedregosa et al., 2011) to develop an empirical relationship between several candidate variables (**Table S2**) and the nitrate loading rate estimated in Stage 1. (Note that for clarity, in the manuscript and in the remainder of the Supplemental Material we use the term ‘GBR-estimated’, ‘GBR-based’, etc., to refer to the empirical relationship between candidate variables and the nitrate loading derived with the GBR; we reserve the general term ‘modeled’ to refer to simulation of nitrate transport described above). Each of the candidate variables listed in **Table S2** is mapped for the entire simulation domain and is thus a potential predictor of nitrate loading for those areas where no nitrate loading data (i.e., groundwater nitrate data) exists. Most of the mapped variables are derived from national-scale datasets [e.g., Cropland Data Layer (USDA, 2014), National Land Cover Dataset, and Soil Survey Geographic Database]. Two

datasets (spatially distributed porosity and recharge) were estimated for the model domain during the flow and transport model development described in the companion paper (Zell et al., 2018). Two additional datasets were derived for this study. First, high resolution Maryland light detection and radar (lidar) elevation data allows identification of field-scale topographic depressions that are the result of drained wetlands. These former wetlands, referred to as 'Delmarva Bays', are often characterized by higher organic content and, therefore, potentially higher rates of soil denitrification (Ator et al., 2012). We consequently generated a map of Delmarva Bays in the model area to use as input for the machine-learning extrapolation. Second, a large commercial nursery in the headwaters of Chesterville Branch is not clearly represented in land use datasets and was consequently mapped and included as a potential explanation of nitrate loading to the water table.

**Table S2.** Mapped variables used as candidate explanatory variables for the GBR-estimated nitrate input function.

<u>Variable Name</u>	<u>Description</u>	<u>Source</u>
CDL_X	Land use category, where X = year	Cropland Data Layer
DelmarvaBays	Topographic indication of drained wetland	This study
Mean_DEM	Mean elevation	Maryland Lidar Dataset
NLCD_X	Land use category, where X = year	National Land Cover Dataset
Nursery	Outline of nursery in Chesterville Branch headwaters	This study
Porosity	Porosity estimated during calibration of flow and transport base model	Zell et al. (2018)
Recharge	Recharge estimated during calibration of flow and transport base model	Zell et al. (2018)
SSURGO_aws_X_wta	Available soil water storage, where X = depth of soil compartment (cm)	Soil Survey Geographic Database (SSURGO)
SSURGO_drclassdcd	Soil drainage class, dominant condition	
SSURGO_drclasswettest	Soil drainage class, wettest condition	
SSURGO_hydclprs	Soil hydric classification	
SSURGO_hydgrpdc	Soil hydrologic group	
SSURGO_pondfreqprs	Ponding frequency	
SSURGO_wtdepannmin	Water table depth, annual minimum	
SSURGO_wtdpaprjunmin	Water table depth, summer minimum	

The GBR-based extrapolation was implemented as follows. At the conclusion of Stage 1a, the model cells in the monitored subdomain were randomly assigned to a training dataset (75% of monitored model cells) and a testing dataset (25% of monitored model cells). The training dataset was used with a 10-fold cross-validation to identify the GBR hyperparameters (e.g., number of trees, tree depth, minimum samples per leaf) that minimized predictive error; the testing dataset was reserved to evaluate the performance of the GBR after the optimal hyperparameters were identified. Finally, the tuned GBR was used to assign a nitrate loading factor to each grid cell in the unmonitored portion of the model domain.

### **S1.C Examination of estimated nitrate inputs to the water table**

The choice of base model and the associated differences in the subsurface flow and transport regime has some effect on the transmission of groundwater nitrate information from the water table to the monitoring wells (**Figure S1**). For example, for the scenario B weighting scheme, the estimated loading field that resulted from the LowBFI scenario had more point locations for which water table inputs approach five times the county-averaged rates (cf. **Figure 3** in the manuscript). These additional point locations of high loading were predominately located in the Chesterville Branch subcatchment, resulting in the higher estimates of loading to that stream (cf. Figure 5 in the manuscript).

While the isolated extreme values visible in **Figure S1** may be considered problematic when using a highly parameterized approach to estimate a field that is expected to be smoothly varying (e.g., hydraulic conductivity), the same is not necessarily the case for the field-scale differentiation of agricultural inputs that we are simulating here. It is additionally important to note that the maximum displayed loading factors are points in the interpolated loading field rather than a field-scale average loading factor. Thus, given the little information available to describe the spatial distribution of loading through time, the heterogeneity and point magnitudes suggested by the various Stage 1 scenarios are not implausible.

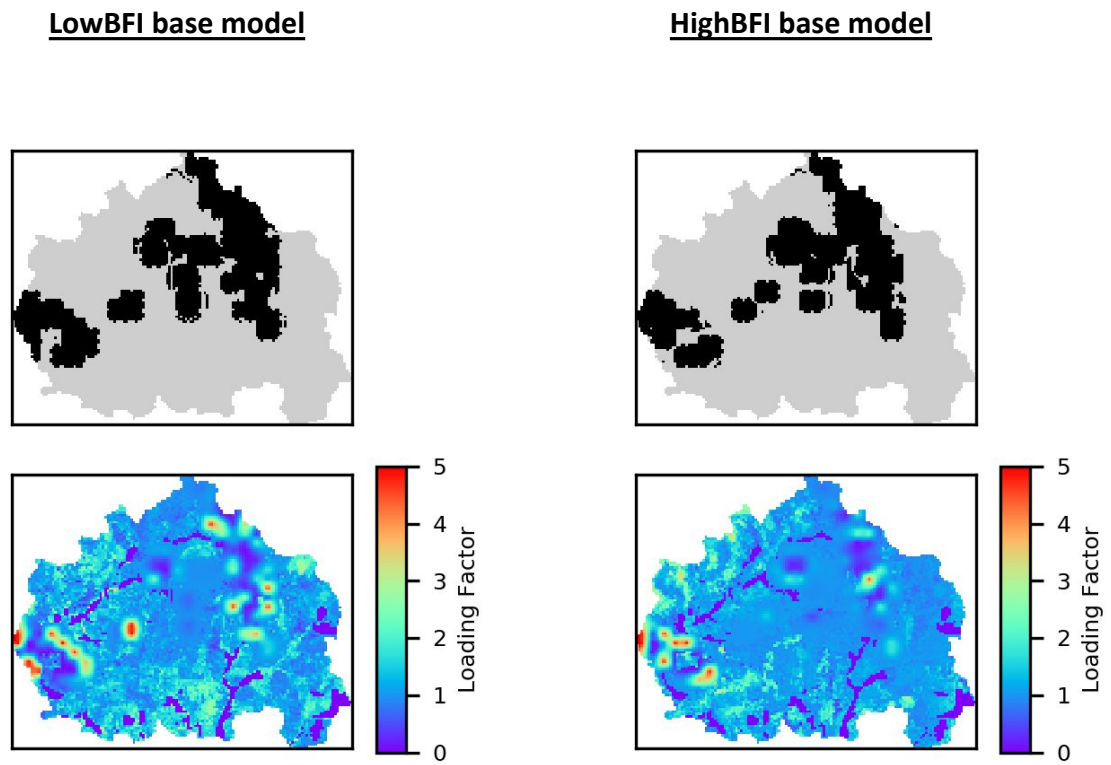


**Figure S1.** Outline of monitored area (top panels) and water table loading factors (bottom panels) for stage 1 Scenario B.

### S1.D Examination of relationships between mapped variables and nitrate loading derived using gradient boosted regression classifier

For the GBR estimators used to extrapolate the spatial distribution of loading from the monitored to the unmonitored areas, the training  $R^2$  ranged from 0.98 to 1.00 and the testing  $R^2$  ranged from 0.60 – 0.72 (**Table S3**). It is important to here emphasize that the purpose of the GBR was not to predict the nitrate loading at any single location in the model domain but rather to represent the likely variance in loading across the landscape without making a priori assumptions about how that variance should be expressed through system parameterization. Representing this variance is in turn important for investigating its effect, if any, on the simulation of the nitrate mass flux seen at the catchment outlet.

**Table S3.** Testing  $R^2$  values for GBR extrapolation of water table loading factors from monitored to unmonitored portions of model domain.

	LowBFI	HighBFI
<b>Weighting scenario A</b>	0.67	0.60
<b>Weighting scenario B</b>	0.70	0.72

While it is outside the scope of this study to fully explore the GBR-formulated relationships between the mapped variables and the water table loading factors, it is interesting to note that the GBR estimator found properties of the flow and transport system (namely, the distribution of recharge and porosity that were estimated during the transport model calibration, as well as topography) more important than other potential explanatory variables (**Figure S2**). Of

secondary importance was land use information derived from the Cropland Data Layer, while the Soil Survey Geographic Database (SSURGO) data played effectively no role in the estimator. Note, however, that cropland may have played a larger role in the regression if all years were aggregated into a single dataset rather than left distributed. The relative insignificance of the SSURGO variables may support our assumption of conservative nitrate behavior, since we would expect that any impacts of soils properties on the inferred loading would be due to interception and removal process (e.g., soil denitrification) rather than variations in the applied loading itself. However, because the GBR detected much more information in the land use data than the soils data, we may assume that the estimated loading factors more represent what was applied at the land surface than what was removed before reaching the water table or en route to an observation location.

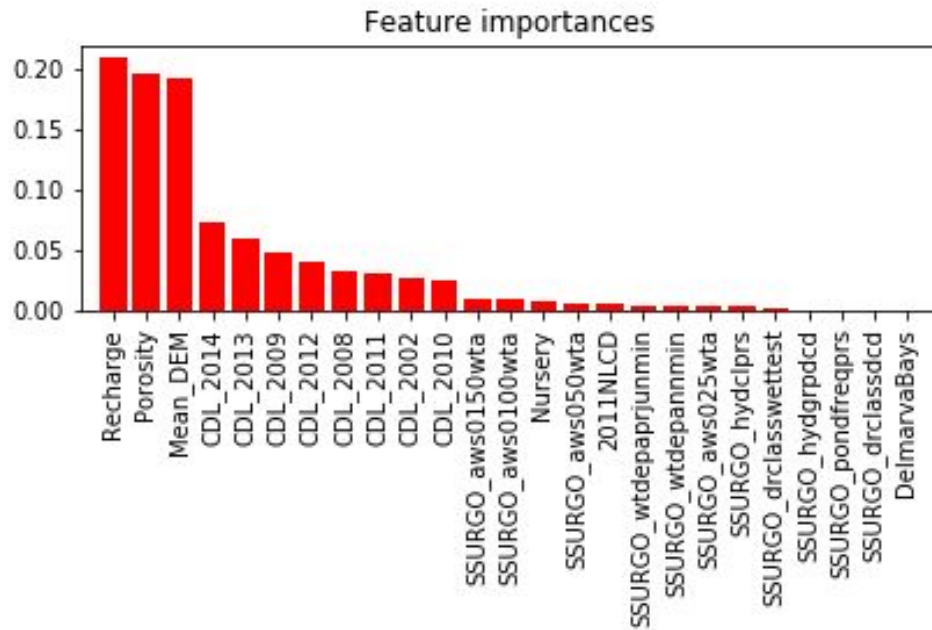


**Figure S2.** GBR-identified importance of explanatory variables to the estimation of nitrate loading factors. See **Table S2** for definition of variables.



## S2 EFFECT OF CALIBRATED TRAVEL TIME SCALING FACTOR ON BASE-FLOW TRAVEL TIME DISTRIBUTIONS (DISCUSSED IN RESULTS SECTION OF MANUSCRIPT)

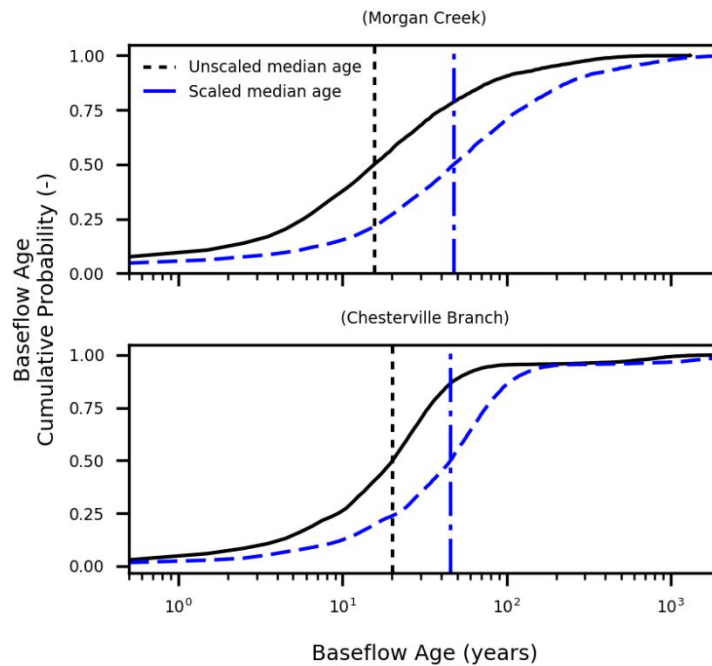


**Figure S3.** The base-flow age empirical cumulative distribution function (ECDF), unadjusted (solid line) and with the TTD scaling factors estimated during the LowBFI Scenario A calibration scenario (dashed line). The vertical lines show the simulated mean base-flow age for the unadjusted (dotted line) and scaled (dash-dot line) TTDs.

## S3 FURTHER DISCUSSION OF STREAM NETWORK CHARACTERISTICS AS POTENTIAL DRIVERS OF CONTRASTING STREAM NITRATE REMOVAL EFFICIENCIES

The Morgan Creek riparian zone is thickly wooded, with tree debris common in the stream channel (Duff et al., 2008). As described in the manuscript, the confining unit which outcrops at the lower reaches may not only account for substantial nitrogen removal through denitrification, but also controls the manner in which discharge enters the main channel. While

Chesterville Branch has not been characterized with the same detail, it is expected that base-flow discharge to Chesterville Branch is via upwelling through the sandy bed sediments with presumably lower denitrification potential, bypassing the riparian zone processing that is an important control in Morgan Creek. This bypass has been observed in other agricultural catchments (Tesoriero et al., 2013). The organic content of the Chesterville Branch bed sediments, and the associated denitrification potential of those sediments (cf. Gu et al., 2008) is not known. Furthermore, a coarse comparison of the stream velocities and associated cross-sectional flow areas (**Figure S4**) suggests that Chesterville Branch has shorter in-stream residence times due to a shorter stream length (**Figure 1** in the manuscript) and higher velocities.

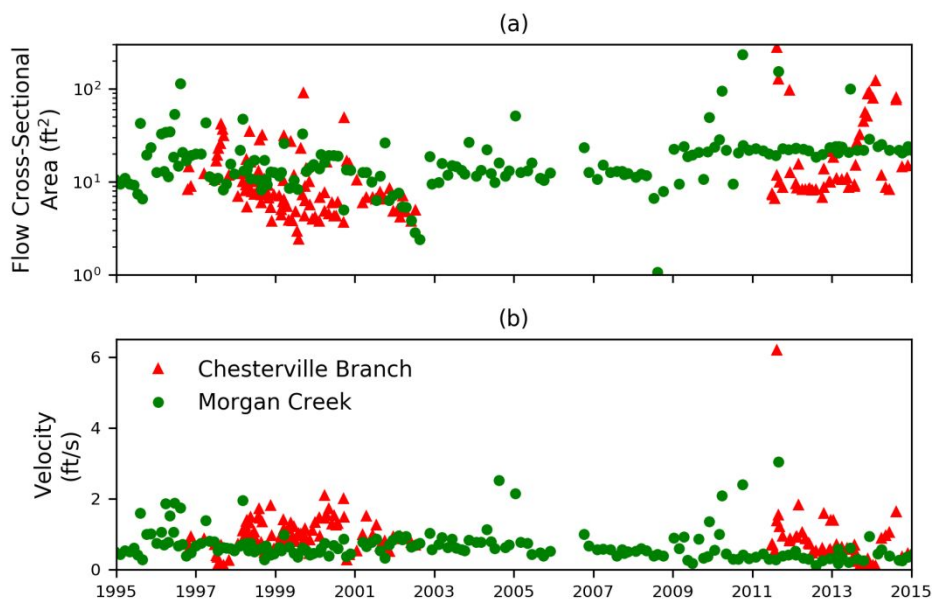


**Figure S4.** Flow characteristics measured at the Morgan Creek and Chesterville Branch stream gages. Each marker represents a field measurement. See **Figure 1** in the manuscript for locations.

Finally, evidence from a small set of synoptic studies suggests that Chesterville Branch headwater concentrations have historically been much higher than headwater concentrations in Morgan Creek (**Figure S5**). These conclusions are likewise tentative because of the few spatially distributed snapshots that include both Morgan Creek and Chesterville Branch but are consistent with the observations and conclusions of Bohlke and Denver (1995). In the early 1990s (i.e., at the time at which the stream networks were simultaneously sampled) surficial aquifer nitrate concentrations in each catchment had nitrate concentrations of 10-20 mg NO<sub>3</sub>-N/L for observation wells near the upstream-most site in both catchments. However, Morgan Creek headwater concentrations were substantially lower than aquifer concentrations, while Chesterville Branch headwater concentrations were not.

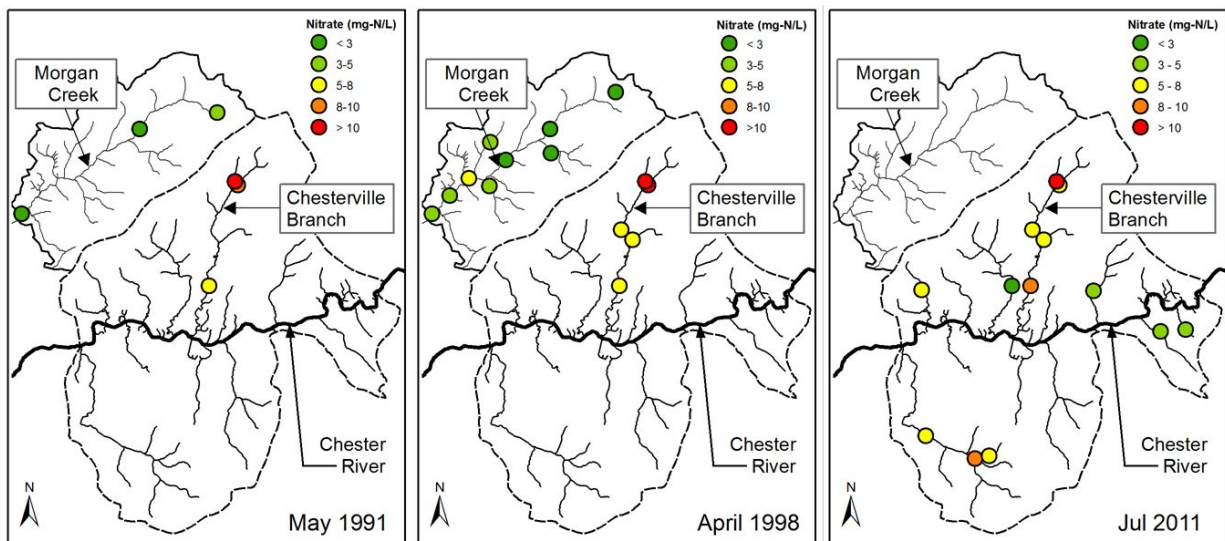


**Figure S5.** Base-flow stream nitrate concentrations from synoptic surface water sampling in Morgan Creek and Chesterville Branch.

#### S4 WORKS CITED

Alexander, R. B., & Smith, R. A. (1990). County-Level estimates of nitrogen and phosphorus fertilizer use in the United States, 1945 to 1985. U.S. Geological Survey Open File Report 90-130. <https://doi.org/10.3133/ofr90130>

Ator, S. W., & Denver, J. M. (2012). Estimating contributions of nitrate and herbicides from groundwater to headwater streams, Northern Atlantic Coastal Plain, United States. *Journal of the American Water Resources Association*, 48(6), 1075-1090.

Böhlke, J. K., & Denver, J. M. (1995). Combined use of groundwater dating, chemical, and isotopic analyses to resolve the history and fate of nitrate contamination in two agricultural watersheds, Atlantic Coastal Plain, Maryland. *Water Resources Research*, 31(9), 2319-2339.

Brakebill, J. W., & Gronberg, J. M. (2017). County-Level Estimates of Nitrogen and Phosphorus from Commercial Fertilizer for the Conterminous United States, 1987-2012: U.S. Geological Survey data release, <https://doi.org/10.5066/F7H41PKX>.

Doherty, J. (2015). PEST, Model-independent parameter estimation: user manual, 5th edn.(and addendum to the PEST manual). Watermark, Brisbane, Australia. Available at [www.pesthomepage.org](http://www.pesthomepage.org).

Duff, J. H., Tesoriero, A. J., Richardson, W. B., Strauss, E. A., & Munn, M. D. (2008). Whole-stream response to nitrate loading in three streams draining agricultural landscapes. *Journal of Environmental Quality*, 37(3), 1133-44.

Fienen, M. N., Muffels, C. T., & Hunt, R. J. (2009). On constraining pilot point calibration with regularization in PEST. *Groundwater*, 47(6), 835-844.

Gronberg, J. M., & Spahr, N. E. (2012). County-level estimates of nitrogen and phosphorus from commercial fertilizer for the conterminous United States, 1987-2006. U.S. Geological Survey Scientific Investigations Report 2012-5207.

Gu, C., Hornberger, G. M., Herman, J. S., & Mills, A. L. (2008). Influence of stream-groundwater interactions in the streambed sediments on NO<sub>3</sub><sup>-</sup> flux to a low-relief coastal stream. *Water Resources Research*, 44(11).

Hancock, T. C., & Brayton, M. J. (2006). Environmental setting of the Morgan Creek Basin, Maryland, 2002-04. US Geological Survey Open File Report 2006-1151.

Murrell, T.S. (2008). Measuring Nutrient Removal, Calculating Nutrient Budgets. *Soil Science: Step-by-step Field Analysis*.

Pedregosa et al (2011). Scikit-learn: Machine Learning in Python. *Journal of Machine Learning Research* (12) 2825-2830.

Sanford, W. E., & Pope, J. P. (2013). Quantifying groundwater's role in delaying improvements to Chesapeake Bay water quality. *Environmental Science and Technology*, 47(23), 13330-13338.

Tesoriero, A.J., Duff, J.H., Saad, D.A., Spahr, N.E. and Wolock, D.M., 2013. Vulnerability of streams to legacy nitrate sources. *Environmental Science and Technology*, v. 47, 3623-3629.

USDA National Agricultural Statistics Service Cropland Data Layer. (2013). Published crop-specific data layer [Online]. Available at <https://nassgeodata.gmu.edu/CropScape/> (accessed March 2014). USDA-NASS, Washington, DC.

U.S. Geological Survey, 2016, USGS water data for the Nation: U.S. Geological Survey National Water Information System database, accessed January 29, 2016, at <https://doi.org/10.5066/F7P55KJN>.

Vinten, A. J. A., Smith, K. A., Burt, T. P., Heathwaite, A. L., & Trudgill, S. T. (1993). Nitrogen cycling in agricultural soils. Nitrate: processes, patterns and management, 39-73.

Welter, D. E., White, J. T., Hunt, R. J., & Doherty, J. E. (2015). Approaches in highly parameterized inversion—PEST++ Version 3, a Parameter ESTimation and uncertainty analysis software suite optimized for large environmental models. U.S. Geological Survey Techniques and Methods 7-C12. <https://doi.org/10.3133/tm7C12>

Zell, W. O., Culver, T. B., & Sanford, W. E. (2018). Prediction uncertainty and data worth assessment for groundwater transport times in an agricultural catchment. *Journal of Hydrology*, 561, 1019-1036.